



Article

Validation of the SCALE/Polaris–PARCS Code Procedure with the ENDF/B-VII.1 AMPX 56-Group Library: Pressurized Water Reactor [†]

Kang Seog Kim ^{1,*}, Byoung-Kyu Jeon ¹, Andrew Ward ², Ugur Mertuyurek ¹ , Matthew Jessee ¹ and William Wieselquist ¹

¹ Nuclear Energy and Fuel Cycle Division, Oak Ridge National Laboratory, One Bethel Valley Road, P.O. Box 2008, MS-6172, Oak Ridge, TN 37831, USA; jeonb@ornl.gov (B.-K.J.); mertuyureku@ornl.gov (U.M.); jesseema@ornl.gov (M.J.); wieselquiswa@ornl.gov (W.W.)

² Nuclear Engineering and Radiological Sciences, University of Michigan, 2355 Bonisteel Boulevard, Ann Arbor, MI 48109, USA; wardam@umich.edu

* Correspondence: kimk1@ornl.gov

[†] This manuscript has been authored by UT-Battelle, LLC, under contract DE-AC05-00OR22725 with the US Department of Energy (DOE). The US government retains and the publisher, by accepting the article for publication, acknowledges that the US government retains a nonexclusive, paid-up, irrevocable, worldwide license to publish or reproduce the published form of this manuscript, or allow others to do so, for US government purposes. DOE will provide public access to these results of federally sponsored research in accordance with the DOE Public Access Plan (<http://energy.gov/downloads/doe-public-access-plan>).

Abstract: This study was conducted to validate the SCALE/Polaris v6.3.0–PARCS v3.4.2 code procedure with the Evaluated Nuclear Data File (ENDF)/B-VII.1 AMPX 56-group library for pressurized water reactor (PWR) analysis, by comparing simulated results with measured data for critical experiments and operating PWRs. Uncertainties of the SCALE/Polaris–PARCS code procedure for PWR analysis were evaluated in the validation for the PWR key nuclear parameters such as critical boron concentrations, reactivity, control bank work, temperature coefficients, and pin and assembly power peaking factors.

Keywords: ENDF/B-VII.1; AMPX 56-group library; pressurized water reactor; SCALE/Polaris; PARCS; validation



Citation: Kim, K.S.; Jeon, B.-K.; Ward, A.; Mertuyurek, U.; Jessee, M.; Wieselquist, W. Validation of the SCALE/Polaris–PARCS Code Procedure with the ENDF/B-VII.1 AMPX 56-Group Library: Pressurized Water Reactor. *J. Nucl. Eng.* **2024**, *5*, 246–259. <https://doi.org/10.3390/jne5030017>

Academic Editor: Dan Gabriel Cacuci

Received: 22 May 2024

Revised: 10 July 2024

Accepted: 17 July 2024

Published: 23 July 2024



Copyright: © 2024 by the authors. Licensee MDPI, Basel, Switzerland. This article is an open access article distributed under the terms and conditions of the Creative Commons Attribution (CC BY) license (<https://creativecommons.org/licenses/by/4.0/>).

1. Introduction

Pressurized water reactor (PWR) physics analysis is usually performed by a conventional two-step procedure based on 2D lattice transport calculations to obtain few-group assembly-homogenized cross sections and then 3D whole-core nodal diffusion calculations. The SCALE [1]/Polaris [2,3]–PARCS [4] two-step procedure was developed by Oak Ridge National Laboratory (ORNL) and the University of Michigan (UM) to support PWR confirmatory analyses by the US Nuclear Regulatory Commission (NRC). The 2D lattice transport code SCALE/Polaris developed by ORNL directly processes the SCALE/AMPX multigroup library and uses the embedded self-shielding method (ESSM) [5] to generate effective resonance self-shielded cross sections. In addition, Polaris adopts the method of characteristics for spatial discretization for the ESSM and eigenvalue calculations and uses SCALE/ORIGEN for depletion calculations. The 3D nodal diffusion code PARCS includes various nodal diffusion solvers for Cartesian and hexagonal meshes and a standalone thermal–hydraulic module for PWR analysis to consider thermal feedback. PARCS supports various PWR simulation capabilities such as depletion, critical boron search, control bank movement, and in-core fuel management. The SCALE/Polaris–PARCS procedure was developed as a substitute for the SCALE/TRITON–PARCS procedure for PWR analysis [6], for better computational efficiency and accuracy and for better user convenience.

Nuclear simulation codes must meet requirements for software quality assurance, and they must be validated for specific applications. Nuclear vendors and institutions

validate their code procedures for PWR analysis by evaluating uncertainties for key nuclear parameters, including hot zero-power (HZP) control bank worths and temperature coefficients, hot full-power (HFP) critical boron concentrations, and pin and assembly power peaking factors. The uncertainties for key nuclear parameters are obtained by comparing the calculated results using an established code procedure with measurement data from critical experiments and PWR power plants' operation. These uncertainties are used for in-core fuel management and safety analysis.

This study focuses on validating the SCALE/Polaris v6.3.0–GenPMAXS [7]–PARCS v3.4.2 code procedure for PWR analysis with the Evaluated Nuclear Data File (ENDF)/B-VII.1 [8] AMPX 56-group library [9,10] without considering epithermal resonance upscattering by evaluating uncertainties for key nuclear parameters. The validation is based on selected critical experiments and reactor benchmarks. The Combustion Engineering (CE) [11,12] and Babcock & Wilcox (B&W)-1810 [13] critical experiments with 11 core configurations were selected for validation. Four PWRs with publicly available design and measured data, including Watts Bar Unit 1 (WBN1) [14,15], Benchmark for Evaluation and Validation of Reactor Simulations (BEAVRS) [16], Surry Unit 1 (SU1) [17], and Turkey Point Unit 3 (TP3) [18], were selected for the reactor benchmark calculations.

Section 2 summarizes the SCALE/Polaris–PARCS code procedure and the benchmark problems and calculations. The benchmark results are summarized and uncertainties for key nuclear parameters are given in Section 3. The Discussion and Conclusions are presented in Sections 4 and 5, respectively.

2. Benchmark Calculations

2.1. SCALE/Polaris–PARCS Procedure

Reactor physics analysis for PWRs is typically performed using a conventional two-step procedure that includes (a) a 2D lattice transport calculation to obtain assembly- and reflector-homogenized few-group cross sections and heterogeneous form factors for pin power distribution, (b) a cross-section functionalization for various reactor states, and (c) a 3D whole-core nodal diffusion calculation with thermal–hydraulic (TH) feedback to estimate the 3D neutron flux distribution and multiplication factor. Figure 1 illustrates the two-step procedure for the PWR physics analysis.

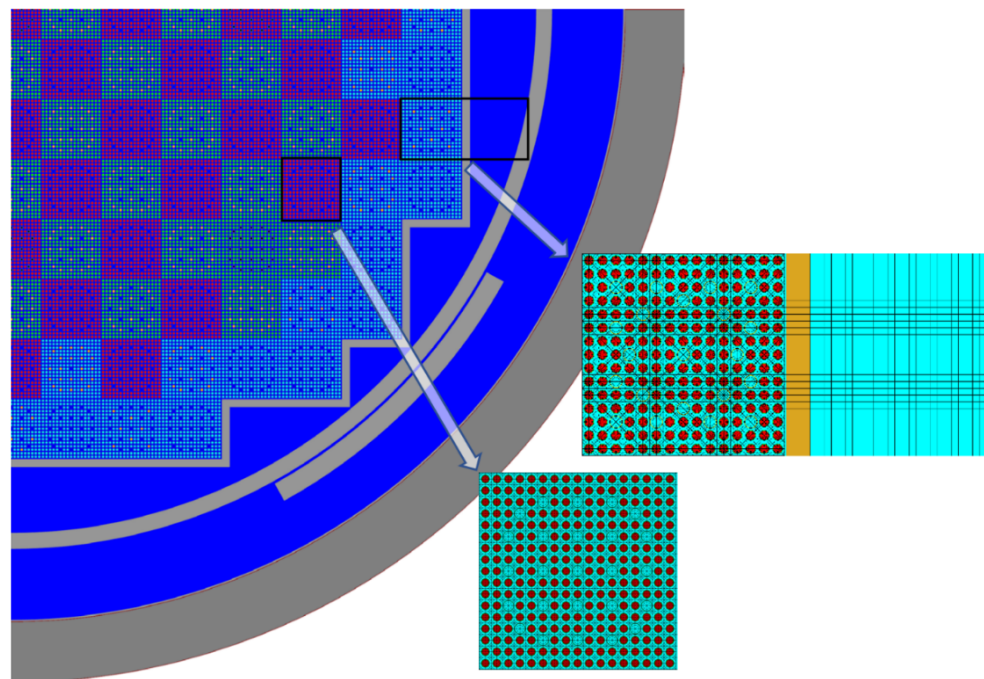


Figure 1. Reactor physics analysis with two-step procedure for PWRs.

Figure 2 illustrates a flowchart of the SCALE/Polaris–PARCS code procedure used to simulate PWRs. Polaris performs the 2D transport calculations for single fuel assemblies and reflector models to obtain homogenized 2-group cross sections for whole-core nodal diffusion calculation. To cover all the possible reactor states, various reference and branch calculations are performed for burnup, moderator and fuel temperatures, moderator density, control rod insertion, and soluble boron concentration. GenPMAXS, developed by UM, uses these Polaris-generated cross sections to prepare cross-section table sets for each type of fuel assembly and reflectors by functionalizing cross sections for various state parameters. Three-dimensional whole-core nodal diffusion calculations are then performed for PWRs using PARCS, from which eigenvalues and 3D flux and power distributions are obtained, and pin powers in an assembly are reconstructed using pin power form factors and nodal powers.

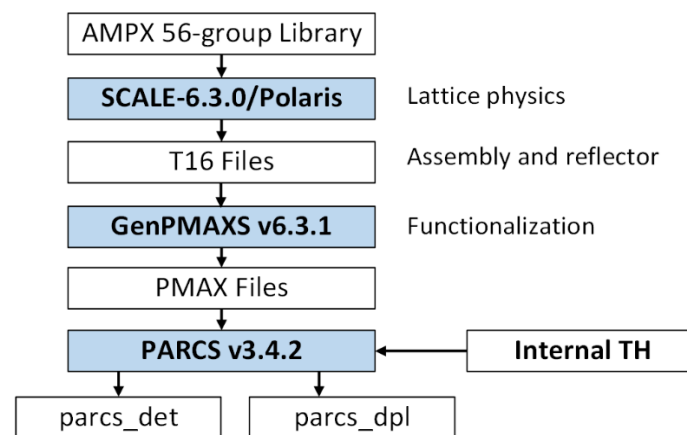


Figure 2. Flowchart of the Polaris–PARCS procedure for PWRs.

2.2. Benchmark Calculations

2.2.1. Overview

Benchmark calculations were performed for two critical experiments and four PWR benchmarks to validate the SCALE/Polaris v6.3.0–PARCS v3.4.2 code procedure with the ENDF/B-VII.1 AMPX 56-group library [9,10]. The final outcomes of the benchmark calculations for validation are uncertainties for key nuclear parameters, including reactivity (or soluble boron concentration), control rod worths, temperature coefficients, and pin and assembly power distributions.

The SCALE/Polaris benchmark calculations were performed for 2 critical experiments with 11 core configurations to evaluate the pin peaking factor uncertainty for PWRs. The critical experiments included five CE core configurations for experiments performed by Westinghouse [11] and six core configurations for experiments performed by B&W [13]. The pin peaking factor uncertainty was evaluated by comparing the measured fission rates and the simulated benchmark results, which can be used in estimating pin power uncertainty in PWRs with statistical summation with assembly power uncertainty. Detailed information and benchmark results are provided in the ORNL technical report ORNL/TM-2023/2979 [19].

Benchmark calculations were performed for four PWR plants, including WBN1 cycles 1–3, BEAVRS cycles 1–2, SU1 cycles 1–2, and TP3 cycles 1–3, using the SCALE/Polaris–PARCS code procedure. The simulated results were compared with the plant-measured data for HZP physics tests, including critical boron concentration, control rod worths and isothermal temperature coefficients (ITCs), and HFP critical boron concentrations and in-core flux (or power) maps. Detailed information for the benchmark calculations and results are provided in the ORNL technical reports ORNL/TM-2023/2981 [15], ORNL/TM-2023/2977 [20], ORNL/TM-2023/3039 [21], and ORNL/TM-2023/3061 [22].

2.2.2. PWR Critical Experiments for Pin Peaking Factor Uncertainty

The 3D pin power distributions in the two-step procedure are reconstructed using the polynomial-expanded nodal powers multiplied by the pin power form factors, obtained from the 2D lattice calculation for each assembly with reflecting boundary condition. In-core detectors located at the specified positions in the PWR and at the central instrumentation tube in each fuel assembly are used to measure flux maps during operation. Sometimes, the measured flux maps are converted into powers based on simulation. Because the in-core detector response does not represent pin flux (or power) but represents more global flux (or power) including neighboring pins, no pin power distribution is measured in commercial PWRs. However, the most critical design limit in PWRs is the enthalpy-rise hot channel factor ($F_{\Delta H}^N$), which is directly related to pin power and departure from nucleate boiling. Therefore, pin power uncertainty for the two-step procedure code procedure must be estimated.

The pin power uncertainty can be obtained indirectly from the assembly power uncertainty and pin peaking factor uncertainty in a fuel assembly. Critical experiments provide measured data for fission rate distribution through gamma scanning for the specified fuel rods in the central fuel assembly of critical cores. Lattice transport codes such as Polaris can perform 2D transport calculations for critical experiment cores, and then, the fission rate distribution can be obtained from the Polaris output. Measured data and calculated results for the normalized fission rate distributions for the central fuel assembly can be compared. Two groups of critical experiments using rod arrays representative of realistic PWR assembly design are adopted in this benchmark calculation. All the critical cores consist of a central fuel assembly surrounded by peripheral fuel pins. The following experiments were considered:

1. The C-E critical experiments were conducted for the Combustion Engineering Company by Westinghouse Electric Company LLC (WH) in 1969. The core represents the C-E 14×14 assembly design [11,12].
2. The B&W-1810 critical experiments were carried out by B&W, Duke Power, and the US Department of Energy (DOE) at B&W's research center. The core represents a $\sim 5 \times 5$ array of either the B&W-1810 15×15 assembly design or the C-E 14×14 assembly design and contains gadolinia-bearing fuel pins. Cores 1, 5, 12, 14, 18, and 20 were selected because they provide the measured fission rates [13].

2.2.3. PWR Benchmark Problems

To perform meaningful benchmark calculations, the PWR core design data, operating history, and measured data must be provided. The PWR core design data include specifications for core configuration, fuel assembly data and loading pattern, and control bank and in-core detector layouts. The operating history must include core pressure, inlet temperature, flow rate, power level, control bank positions, and critical boron concentrations. The measured data for the HZP physics test include critical boron concentrations, control bank worths, ITCs, boron worths, and in-core detector responses. The HFP measured data include critical boron concentrations and in-core detector responses at the specified burnup points. Publicly available PWR plant data and documents were collected for the Polaris–PARCS benchmark calculations.

Reports from the Electric Power Research Institute (EPRI) provide detailed information for SU1 [17] and TP3 [18]. Detailed data for WBN1 come from the Consortium for Advanced Simulation of Light Water Reactors (CASL) report (CASL-U-2012-031-004) [14]. However, the CASL report provides mostly plant and core design data but no measured data; WBN1 provided the measured data with different files to CASL. The ORNL technical report [15] includes detailed measured data which can be used in benchmark calculations. The Massachusetts Institute of Technology report [16] for BEAVRS provides detailed data for core design, operating history, and measured data, which might be a best standard for benchmark calculations. Table 1 provides the specifications of the four selected PWR plants.

Table 1. Specifications of the PWR plants.

Parameter	Watts Bar Unit 1	BEAVRS	Surry Unit 1	Turkey Point 3
Core power (MW _{th})	3411	3411	2441	2200
Operating pressure (psia)	2250	2250	2250	2250
Core flow rate (10 ⁶ kg/h)	59.738	61.5	45.8	44.0
Inlet temperature (°C)	291.85	292.89	293.33	282.22
Number of assemblies	193	193	157	157
Initial core loading (MTU)	88.8	81.8	70.0	70.4
Pin lattice configuration	17 × 17	17 × 17	15 × 15	15 × 15
Active fuel length (cm)	365.76	365.76	366.903	365.76
Number of fuel rods	264	264	204	204
Number of spacer grids	6 Zr-4, 2 Inc-718	6 Zr-4, 2 Inc-718	7 Inc-718	7 Inc-718
Assembly pitch (cm)	21.50	21.50364	21.50364	21.50364
Pin pitch (cm)	1.26	1.25984	1.43	1.43
Fuel pellet radius (cm)	0.4096	0.39218	0.46469	0.46469
Cladding inner/outer radius (cm)	0.4180/0.4570	0.40005/0.45720	0.47422/0.53594	0.47422/0.53594
Number of control banks	57	57	53	53
Control rod material	B ₄ C/AgInCd	B ₄ C/AgInCd	AgInCd	AgInCd
Burnable poison material	Pyrex, IFBA ^a , WABA ^b	Pyrex	Pyrex	Pyrex
In-core detector	Fission chamber	Fission chamber	Fission chamber	Fission chamber

^a IFBA = integrated fuel burnable absorber. ^b WABA = wet annular burnable absorber.

2.2.4. Benchmark Calculations for PWR Plants

The SCALE/Polaris inputs were prepared using the design data to process assembly-homogenized 2-group cross sections for whole-core nodal diffusion calculations. To cover all the possible reactor states, the 2-group cross sections were tabulated as a function of burnup, moderator and fuel temperatures, moderator density, soluble boron concentration, and control rods. Polaris was used to perform depletion calculations for 16 reference cases with and without spacer grids. To complete the functionalization of the cross-section table sets, various branch calculations should be performed at each burnup point for each reference case. The number of state points for the Polaris transport calculation for each assembly with and without burnable poison (BP) was as follows:

- No-BP assembly: 8 (reference case) × 2 (spacer grid) × 21 (burnup) × 45 (branch) = 15,120;
- BP assembly: 8 (reference case) × 2 (spacer grid) × 21 (burnup) × 36 (branch) = 12,096.

Very expensive computing time is required to prepare a cross-section set for each fuel assembly type; this process needs to be improved in the future for better computational efficiency. The Polaris calculations are performed for radial, top, and bottom reflectors sided by a single fuel assembly without depletion calculation but with branch calculations for moderator temperature, moderator densities, and boron concentrations. Figure 1 provides illustrations of typical Polaris fuel assembly and reflector models. Polaris saves all the required information for the nodal diffusion calculation on so-called T16 files. Although the PWR plant, fuel, and core design data are provided at room temperature conditions, the benchmark calculations are performed for the HZP and HFP temperature conditions. Therefore, all the geometry and composition data must be thermally expanded at hot temperatures.

Cross-section table sets were prepared for various types of fuel assemblies and reflectors using GenPMAXS v6.3.1. If there is axial heterogeneity from the spacer grid, burnable poisons, and axial blanket, then different types of cross-section table sets must be generated. Although only one Polaris fuel-to-reflector model is used for radial reflector cross sections, various radial reflector cross-section sets are generated according to various fuel-to-reflector configurations in the reactor core.

Whole-core 3D nodal diffusion calculations were performed using PARCS v3.4.2. The PARCS input requires various types of information for core calculations, such as thermal power, inlet temperature, coolant flow rate, fuel assembly loading pattern, 3D geometry specification, control bank and in-core detector layouts, and cross-section assignment to

each node. Nodal diffusion calculations are performed at various given reactor conditions, including reactor power, flow rate, control bank movement, and burnup for depletion. It is noted that BPs such as Pyrex and wet annular burnable absorber are treated similarly to control rods. When a PARCS calculation is completed, detailed information is saved in a history file that can be used in fuel shuffling. The summarized result can be found in the *.dpl file, and the in-core detector response result is printed in the *.det file.

3. Results

3.1. Critical Experiment Benchmark Results

The fission rates calculated with Polaris were compared with the measured rates. Each set of data was normalized to the average of the central quarter fuel assembly. The measurements were obtained from Tables 5.1 through 5.5 of Kim’s technical report [12] for the CE critical experiments and Tables 4–6 through 4–20 of Newman’s report [13] for the B&W-1810 critical experiments. The measurement standard deviation (S_m) could be obtained from the symmetric measurements relative to the average.

Table 2 summarizes the total (S_d), measurement, and calculation (S_c) standard deviations and degrees of freedom (DOFs) for the total (F_d) and measurement (F_m) on the pin peaking factors for each critical experiment, followed by the estimation of the pooled standard deviation and calculation uncertainty on the pin peaking factor. For each experiment, the DOF for calculation (F_c) is calculated from the following relationship:

$$S_{d/F_d}^4 = S_{c/F_c}^4 + S_{m/F_m}^4 \tag{1}$$

Table 2. Pin peaking factor uncertainty based on parametric statistical analysis.

Critical Experiments		S_d	F_d	S_m	F_m	S_c	F_c
C12	CE12	0.947	21	1.040	19	–	–
C32	CE32	1.076	21	0.661	19	0.849	10
C43	CE43	0.900	21	0.867	19	0.240	2
C53	CE53	0.616	21	0.988	19	–	–
C56	CE56	0.679	21	0.594	19	0.329	3
CE All		0.861	0.861	0.848	95	0.699	15
B01	B&W01	0.504	25	0.168	64	0.475	20
B05	B&W05	0.637	25	0.381	64	0.510	11
B12	B&W12	0.730	25	0.435	64	0.587	11
B14	B&W14	1.026	25	0.491	64	0.900	15
B18	B&W18	1.012	28.5	0.772	64	0.655	6
B20	B&W20	1.152	28.5	0.584	64	0.993	16
BAW All		0.886	157	0.507	384	0.728	79
S_p (All)		0.876	262	0.590	479	0.724	94
$K_{95 \times 95}$		1.811		1.766		1.937	
$K_{95 \times 95} S_p$		1.586		1.043		1.402	

The overall standard deviation (S_p) can be obtained as the weighted average of the individual standard deviations:

$$S_p^2 = \frac{\sum_{i=1}^J v_i S_i^2}{v_e} \text{ and } v_e = \sum_{i=1}^J v_i, \tag{2}$$

where ν_i is the number of DOFs for the case i , and J is the number of cases. Table 2 shows that the statistical calculation uncertainty (KS) is $\pm 1.586\%$ using the parametric statistics method where K is a one-sided tolerance limit [23]. The pin peaking factor uncertainty using the parametric statistics method was determined directly from the total tolerance limit; this approach was selected for greater conservatism without considering measurement uncertainty. Although this tolerance limit is taken, this value is still comparable with those of other transport lattice codes. As shown in Figure 3, the $(-)$ uncertainty (KS_c) from simple counting is -1.60% , which is more negative than the statistical uncertainty -1.586% . The statistical uncertainty can be obtained using the nonparametric statistics method for nonnormal distribution with the following equation:

$$P(X_p \leq X_j) = \sum_{k=0}^{j-1} \binom{N}{k} 0.95^k 0.05^{N-k}, \text{ and } X_1 \leq X_2 \leq \dots \leq X_p \leq X_j \leq \dots \leq X_N, \quad (3)$$

where P is a probability, and N denotes the number of data points. When j is found for $P(X_p \leq X_j) \geq 0.95$, the X_j will be a tolerance limit with 95×95 probability and confidence level. Because the number of data points is 273, j will be 264. Therefore, the $(-)$ and $(+)$ uncertainties (KS_{non}) from the nonparametric statistical method are -1.90% and 1.57% , respectively. Therefore, to be the most conservative, the resulting calculation uncertainty was determined to be $\pm 1.90\%$.

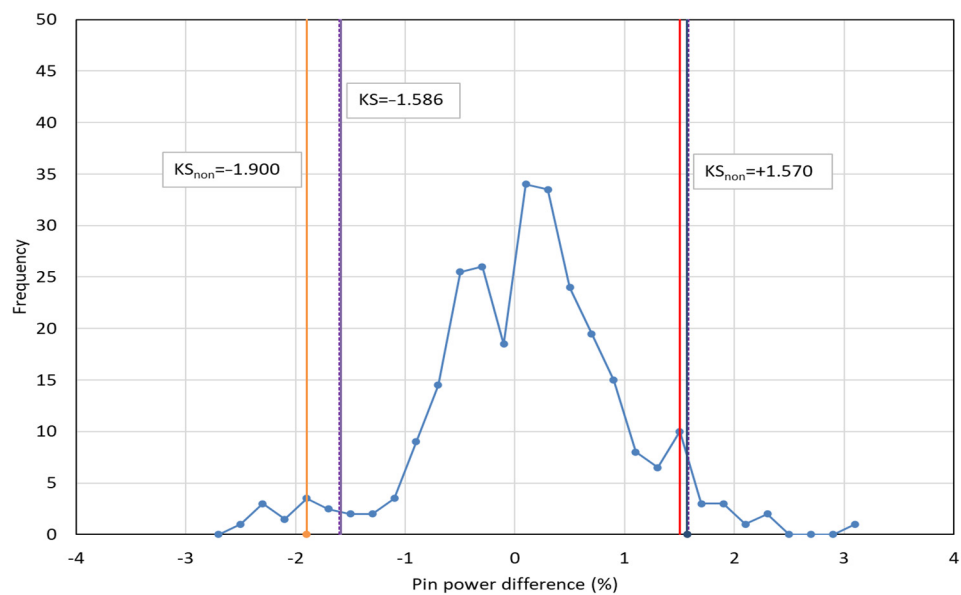


Figure 3. Pin peaking factor uncertainty.

3.2. PWR Benchmark Results

3.2.1. Hot Zero-Power Physics Tests

Table 3 compares the measured data and the calculated results of the control bank worths, critical boron concentrations, ITCs, and boron worth in the WBN1, BEAVRS, and TP3 HZP physics tests. The EPRI report for SU1 [17] does not provide the HZP physics test result. The calculated results for cycles 2–3 could not be included in the table because PARCS has limited capability for modeling the discharge of Pyrex BPs after cycle 1. Because the amount of measured data and the number of calculated results are not sufficient to obtain a statistically meaningful uncertainty, the Polaris–PARCS procedure must be improved to resolve the BP discharge capability and to collect more HZP physics test results. Detailed information and results are provided in the ORNL technical reports for individual PWRs, including ORNL/TM-2023/2981 [15], ORNL/TM-2023/2977 [20], ORNL/TM-2023/3039 [21], and ORNL/TM-2023/3061 [22].

Table 3. Comparisons of the HZP control bank worth, ITC, and boron worth.

Reactor	Case	Critical Boron (ppm)			Control Bank Worth (pcm)			ITC (pcm/°F)			Boron Worth (pcm/ppm)		
		M ^a	C ^b	C-M	M	C	C-M	M	C	C-M	M	C	C-M
WBN1	ARO ^c	1291	1281	-10				-2.17	-3.39	-1.22	-10.77	-10.18	0.59
	A				843	977	134						
	B				879	840	-39						
	C				951	1031	80						
	D				1342	1450	108						
	SA				435	421	-14						
	SB				1056	1077	21						
	SC				480	458	-22						
	SD				480	458	-22						
All				6466	6713	247							
BEAVRS	ARO	975	958	-17				-1.75	-2.03	-0.28			
	D (ARO)	902	896	-6	788	794	6	-4.65	-3.49	1.16			
	C (D in)	810	795	-15	1203	1276	73	-8.01	-8.27	-0.26			
	B (D+C in)		703		1171	1213	42						
	A (D+C+B in)	686	655	-31	548	615	67						
	SE (D+C+B+A in)		613		461	526	65						
	SD (D+C+B+A+SE in)		552		772	756	-16						
	SC (D+C+B+A+SE+SD in)	508	464	-44	1099	1112	13						
TP3	ARO		1168										
	D (ARO)		1089		894	898	4				-14.1	-11.4	2.7
	C (D in)		963		1496	1435	-61				-12.0	-11.9	0.1
	B (C+D in)		885		1055	935	-120				-15.4	-13.5	1.9
	A (B+C+D in)		732		1856	1775	-81				-12.1	-12.2	-0.1

^a Measured. ^b Calculated. ^c All rods out.

3.2.2. Hot Full-Power Critical Boron Concentrations and Reactivities

Comparisons of the HFP critical boron concentrations and reactivities are illustrated in Figures 4 and 5, respectively, and are used in statistical analysis to obtain uncertainties for critical boron concentration and reactivity. The reactivity differences were obtained using the differences of the critical boron concentrations between the measurement and simulations with the calculated burnup-dependent boron worths for each PWR. Detailed information and results are provided in the ORNL technical reports for individual PWRs, as specified in Section 3.2.1.

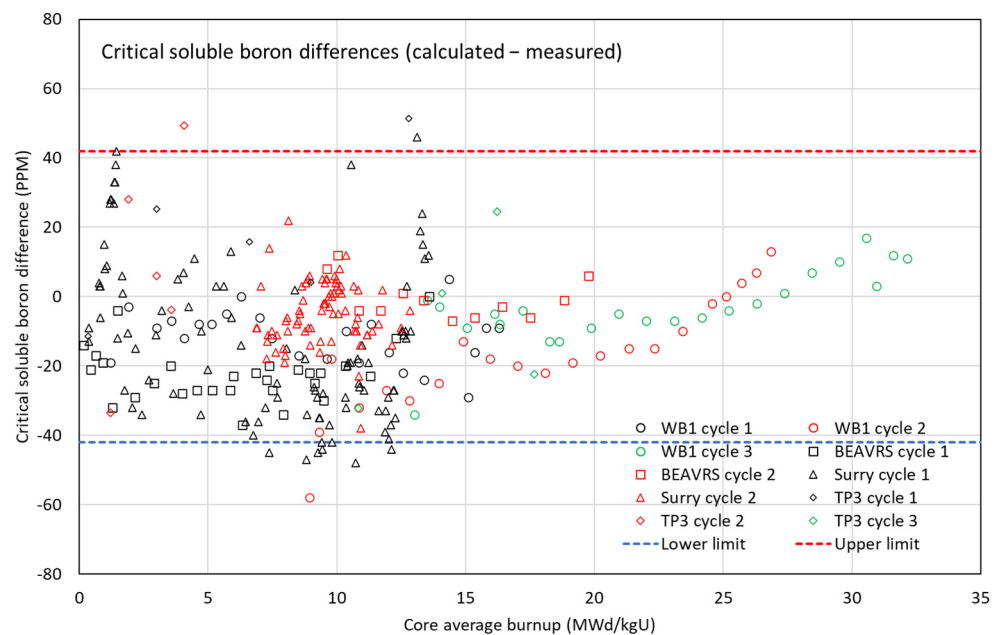


Figure 4. Differences in the critical boron concentrations between measurement and simulation.

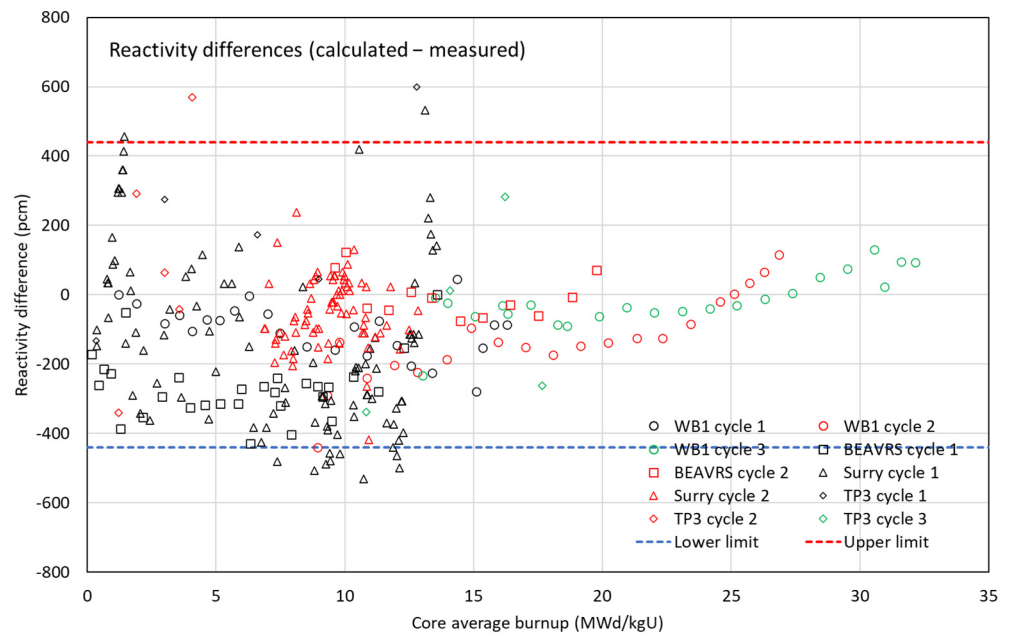


Figure 5. Reactivity differences between measurement and simulation.

3.2.3. Hot Full-Power In-Core Flux Maps

Comparisons of the HFP flux (or power for SU1) maps are illustrated in Figure 6 for WBN1, BEAVRS, SU1, and TP3. These comparisons are used in statistical analysis to obtain uncertainty for power distributions. The root mean square (RMS) errors for the measured flux maps obtained using the measured data at symmetric detector positions were obtained for WBN1 and BEAVRS and can be considered in estimating the calculation uncertainty for the flux map data. Detailed information and results are provided in the ORNL technical reports for specific PWRs.

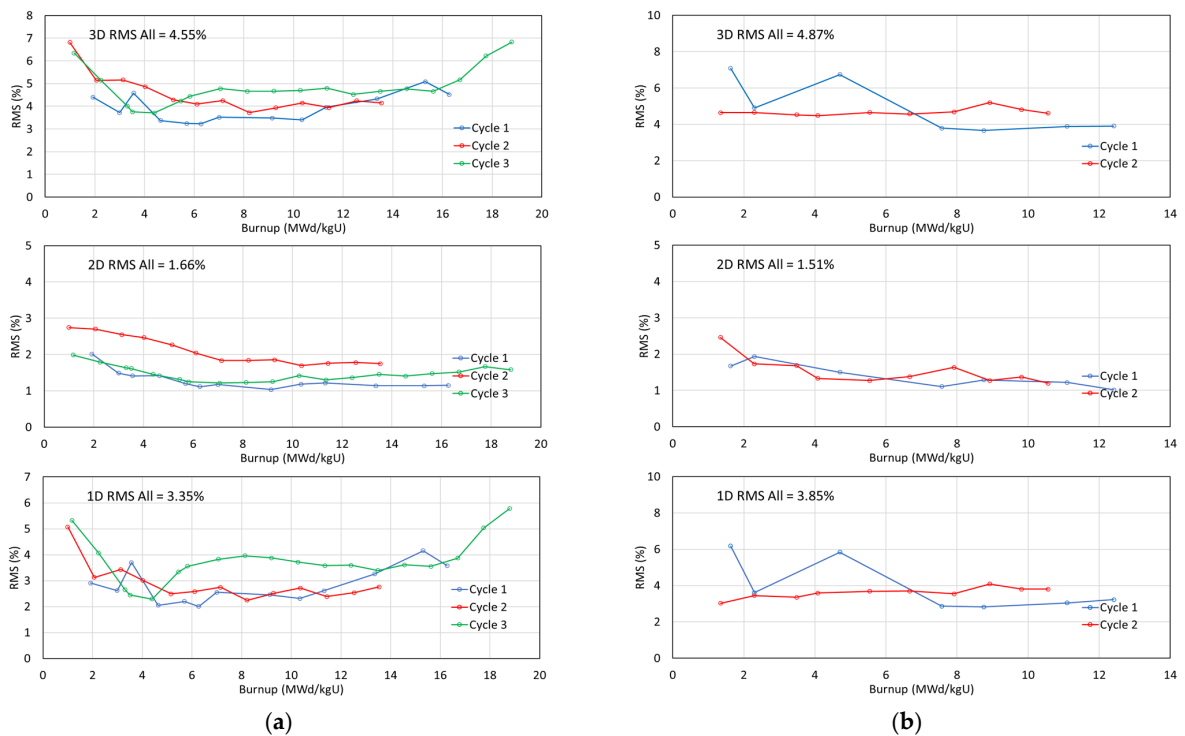


Figure 6. Cont.

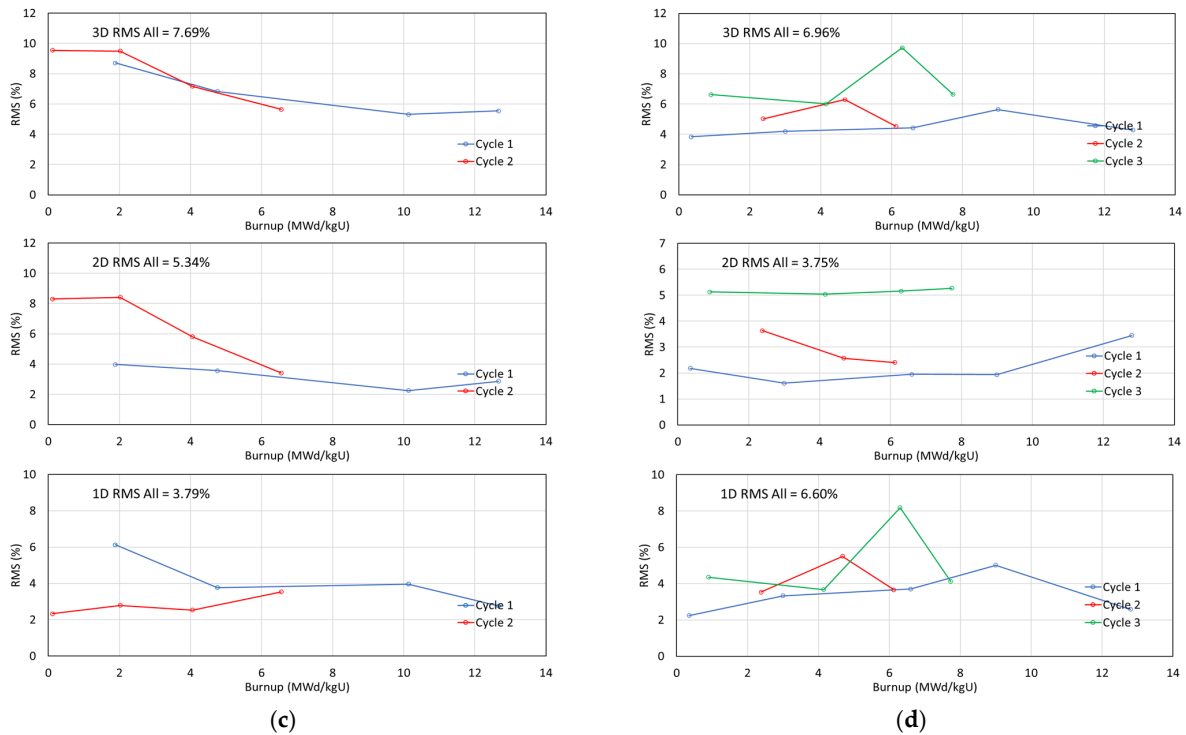


Figure 6. Comparison of the HFP flux maps. (a) WBN1. (b) BEAVRS. (c) SU1. (d) TP3.

3.3. Uncertainty Evaluation

Statistical analysis was performed using three different methods: (a) a parametric statistical method, (b) a nonparametric statistical method, and (c) a simple bound method. The parametric statistical method was introduced in Section 3.1 and includes the following steps: (a) perform normality test, (b) obtain standard deviation (S_d) for the differences between the measurement and simulation, (c) read 95×95 one-sided tolerance limit ($K_{95 \times 95}$) for DOF from the reference [23], and (d) obtain uncertainty ($K_{95 \times 95} S_d$) with 95×95 probability/confidence level by multiplying the one-sided tolerance limit with the standard deviation. The nonparametric statistical method to obtain uncertainty (KS_{non}) is also introduced in Section 3.1 and can typically be used for the cases failed in normality tests. The simple bound method is the use of maximum or minimum values as the uncertainty. Table 4 summarizes the statistical analysis for the PWR key nuclear parameters.

Typically, the uncertainty from nonparametric statistics is more conservative than the uncertainty from parametric statistics. The most conservative uncertainty was selected for this effort from various uncertainties obtained from various statistical methods. Table 4 summarizes the uncertainty analysis for the PWR key nuclear parameters.

Parametric and nonparametric statistical analyses were performed for the pin peaking factor uncertainty, as detailed in Section 3.1. The uncertainty from nonparametric statistics is more conservative than the uncertainty from parametric statistics, so the final pin peaking factor uncertainty (KS) is $\pm 1.90\%$.

Not enough data were available for the HZP physics tests. Parametric statistics was performed only for control rod worths. Because the uncertainty for control rod worth from parametric statistics is larger than the uncertainty from the bound approach, the final uncertainty for control rod worth is $\pm 18.0\%$. The uncertainties for ITC and boron worth were determined to be ± 1.22 pcm/ $^{\circ}$ F and $\pm 19.1\%$, respectively, using the bound method. These uncertainties for control rod worth, ITC, and boron worth must be updated by collecting more measured data and resolving the capability limitation issue for the BP discharge in PARCS.

An ~10 ppm bias exists for the critical boron concentration. A decision was made to neglect the bias and obtain the uncertainty for critical boron concentration using parametric and nonparametric statistical methods. Because the uncertainty obtained by nonparametric statistics is more conservative, the final uncertainties are ±41 ppm for critical boron concentration and ±440 pcm for reactivity. Figures 4 and 5 illustrate the distribution of the differences of critical boron concentrations and reactivities between the measurement and simulation.

There are many data points for the HFP flux maps, and when normalized to one, they can be assumed to be a normal distribution. Therefore, only a parametric statistical analysis was performed. The measurement uncertainty ($K_{95 \times 95} S_m$) can be calculated using the measured flux map data at the symmetric in-core detector positions. The calculation uncertainty ($K_{95 \times 95} S_c$) can be calculated using Equations (1) and (2). The final uncertainties for 3D, 2D, and 1D flux maps are ±8.1%, ±3.7% and ±7.1%. The uncertainties for 3D and 2D flux maps can be uncertainties for 3D and axially integrated 2D fuel assembly power distributions, which can be combined with the pin peaking uncertainty to obtain 3D and 2D pin power uncertainties. The final uncertainties for 3D and 2D pin power distributions are ±8.3% and ±4.2%, respectively.

Table 4. Uncertainties for the PWR key nuclear parameters.

Method	Item	Pin Peaking Factor (%)	HZP				HFP			
			Rod Worth (%)	ITC (pcm/°F)	Boron Worth (%)	Boron (ppm)	$\Delta\rho$ (pcm)	3D	Flux Map (%) 2D	1D
Parametric statistics (difference)	S_d	—	—	—	—	—	—	5.20	2.29	4.17
	Average cases	—	—	—	—	—	—	—	—	—
	$K_{95 \times 95}$	—	—	—	—	—	—	120,552	4014	2600
	$K_{95 \times 95} S_d$	—	—	—	—	—	—	1.645	1.687	1.696
Parametric statistics (measurement)	S_m	—	—	—	—	—	—	±8.5	±3.9	±7.1
	Average cases	—	—	—	—	—	—	—	—	—
	$K_{95 \times 95}$	—	—	—	—	—	—	1.67	0.75	—
	$K_{95 \times 95} S_m$	—	—	—	—	—	—	83,644	2811	—
Parametric statistics (calculation)	S_c	0.886	7.4	1.0	11.7	20.3	219	4.92	2.17	—
	Average cases	—	1.9	−0.15	−7.4	−9.9	−100	—	—	—
	$K_{95 \times 95}$	273	20	4	5	299	299	98,471	3257	—
	$K_{95 \times 95} S_c$	±1.586	±18.0	—	—	±37	±393	±8.1	±3.7	—
Nonparametric statistics	Upper	1.57	—	—	—	28	306	—	—	—
	Lower	−1.90	—	—	—	−41	−440	—	—	—
	KS_{non}	±1.90	—	—	—	±41	±440	—	—	—
Bound	Maximum	—	15.9	1.16	0.8	—	—	—	—	—
	Minimum	—	−11.4	−1.22	−19.1	—	—	—	—	—
	KS	—	±15.9	±1.22	±19.1	—	—	—	—	—
Final	KS	±1.90%	±18.0	±1.22	±19.1	±41	±440	±8.1	±3.7	±7.1

4. Discussion

Flux map comparison. Table 5 compares the total 3D, 2D, and 1D flux map RMS errors for WBN1 between the high-fidelity code VERA [24] and the SCALE/Polaris-PARCS results compared with the measured data. Although the 2D RMS errors of the Polaris-PARCS results are comparable with the RMS errors of the VERA results, there is a ~1.5% difference in the 1D and 3D RMS errors between the VERA and Polaris-PARCS results. This indicates that the axial reflector models for Polaris-PARCS need to be improved. Figure 7 compares the 1D axial flux maps between measurement and simulation at burnups 1.92 and 13.36 MWd/kgU for the WBN1 cycle 1. This figure indicates an axial power tilt, likely resulting from poor axial reflector cross sections.

Enthalpy-rise hot channel factors. Figure 8 shows the enthalpy-rise hot channel factors ($F_{\Delta H}^N$) as a function of burnup; some cases do not satisfy the limit of 1.435 considering 8% uncertainty, but they do satisfy the limit of 1.55 without considering uncertainty. The $F_{\Delta H}^N$ limit is obtained from the departure from nucleate boiling. This violation might come

from no gamma smeared pin power form factors and should be addressed by performing a neutron-gamma coupled calculation and considering gamma energy deposition.

Table 5. Comparison of flux maps for WBN1 between VERA and Polaris-PARCS.

Cycle	VERA RMS %			Polaris-PARCS RMS %		
	3D	2D	1D	3D	2D	1D
1	3.0	1.3	1.8	4.0	1.3	2.9
2	3.2	1.9	1.4	4.6	2.1	3.0
3	3.3	1.5	2.4	4.9	1.5	3.9

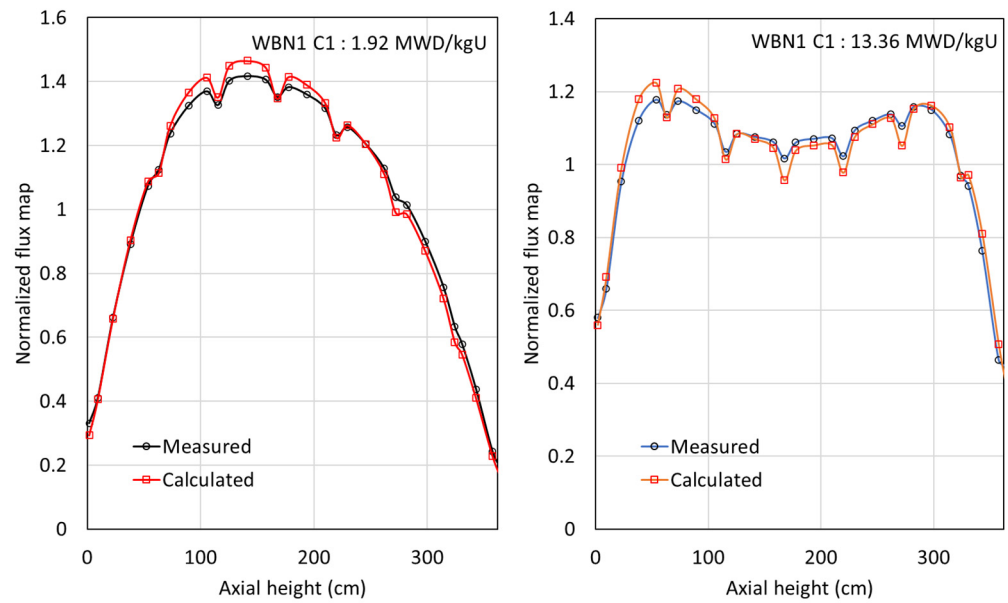


Figure 7. Axial 1D flux map comparison for WBN1 cycle 1.

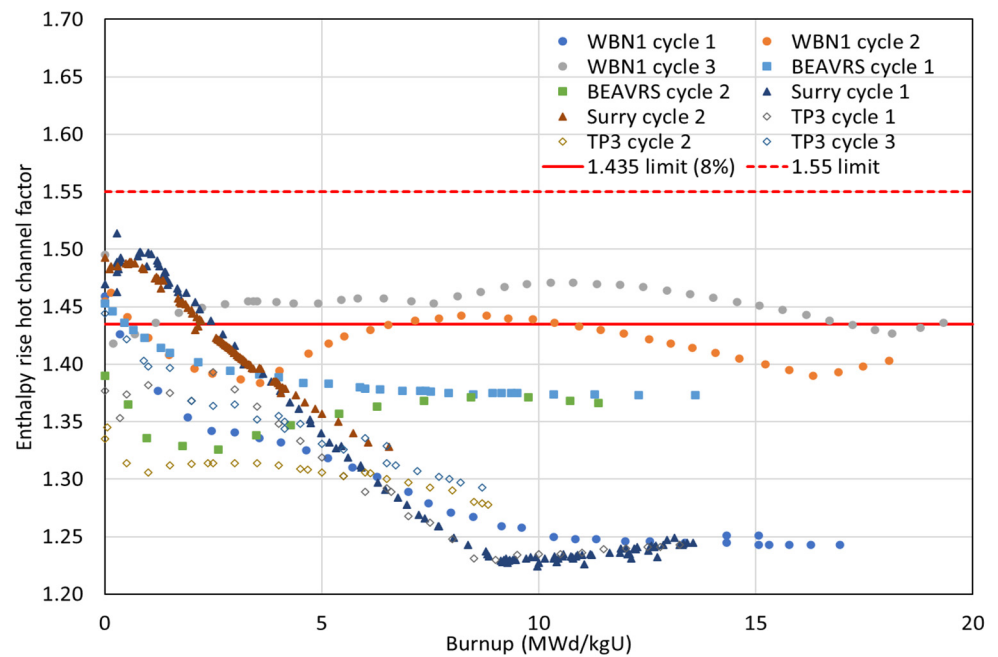


Figure 8. Enthalpy-rise hot channel factors.

Capability limitations in PARCS v3.4.2. PARCS v3.4.2 will need to improve to address the following capability limitations and instabilities for PWR physics analysis:

- Limitation in the capability of discharging BPs such as Pyrex after a cycle.
- Different PMAX file assignment and burnups for assembly quadrants.
- Limitation on assembly rotation to consider quadrant-dependent burnups.
- PARCS does not support 2×2 nodes for each fuel assembly, which would limit treating the fuel assembly with asymmetric BPs and quadrant-dependent burnup because of the different surrounding fuel assemblies. The 2×2 node capability with different cross sections and burnups would enhance the overall accuracy of the Polaris–PARCS code procedure.

5. Conclusions

The objective of this validation study for the SCALE/Polaris v6.3.0–PARCS v3.4.2 code procedure with the ENDF/B-VII.1 AMPX 56-group library was to assess uncertainties for PWR key nuclear parameters, such as critical boron concentration, reactivity, temperature reactivity coefficients, control rod worth, and pin and assembly power peaking factors.

This validation of the SCALE/Polaris–PARCS code procedure for PWR analysis was a successful first trial. However, the validation study must be improved to address the following identified issues:

- Incomplete analysis procedure, especially for radial and axial reflector cross sections;
- Limitation of the SCALE/Polaris–PARCS modeling capability for the BP discharge after cycle;
- Lack of sufficiently reliable PWR plant design and measured data.

The Polaris–PARCS procedure must be improved to provide a standard, robust procedure to users and to support NRC's confirmatory analysis. More PWR plant design and measured data must be collected and included in the validation to be more statistically meaningful. In addition, other versions of ENDF/B, such as ENDF/B-VIII.0 and VIII.1, must be investigated to assess the impact of nuclear data on uncertainties for the PWR key nuclear parameters.

Author Contributions: Conceptualization, K.S.K.; formal analysis, K.S.K., B.-K.J., U.M. and A.W.; investigation, K.S.K., M.J. and B.-K.J.; writing—original draft preparation, K.S.K.; writing—review and editing, W.W.; supervision, W.W.; project administration, W.W.; funding acquisition, W.W. All authors have read and agreed to the published version of the manuscript.

Funding: This research was funded by the US Nuclear Regulatory Commission Office of Research contract number 31310019N0008.

Data Availability Statement: The data presented in this study are available on request from the corresponding author.

Conflicts of Interest: The authors declare no conflicts of interest.

References

1. Wieselquist, W.A.; Lefebvre, R.A. (Eds.) *SCALE 6.3.1 User Manual*; ORNL/TM-SCALE-6.3.1; UT-Battelle, LLC, Oak Ridge National Laboratory: Oak Ridge, TN, USA, 2023. Available online: <https://scale-manual.ornl.gov/> (accessed on 1 May 2024).
2. Jessee, M.A.; Wieselquist, W.A.; Mertyurek, U.; Kim, K.S.; Evans, T.M.; Hamilton, S.P. Lattice physics calculations using the embedded self-shielding method in Polaris, Part I: Methods and implementation. *Ann. Nucl. Energ.* **2021**, *150*, 107829. [CrossRef]
3. Mertyurek, U.; Jessee, M.A.; Betzler, B.R. Lattice Physics calculations using the embedded self-shielding method in Polaris, Part II: Benchmark assessment. *Ann. Nucl. Energ.* **2021**, *150*, 107830. [CrossRef]
4. Downar, T.; Xu, Y.; Seker, V. *PARCS NRC–v3.4.2 Volume I: Input Manual*; University of Michigan: Ann Arbor, MI, USA, 2022.
5. Williams, M.L.; Kim, K.S. The Embedded Self-Shielding Method. In Proceedings of the PHYSOR 2012, Knoxville, TN, USA, 15–20 April 2012.
6. Ade, B.J.; Frankl, I. *SCALE/TRITON Primer: A Primer for Light Water Reactor Lattice Physics Calculations*; NUREG/CR-7041, ORNL/TM-2011/21; Oak Ridge National Laboratory: Oak Ridge, TN, USA, 2012.
7. Ward, A.; Xu, Y.; Downar, T. *GenPMAXS—v6.3.1 Release Code for Generating the PARCS Cross Section Interface File PMAXS*; University of Michigan: Ann Arbor, MI, USA, 2021.

8. Chadwick, M.B.; Herman, M.; Obložinský, P.; Dunn, M.E.; Danon, Y.; Kahler, A.C.; Smith, D.L.; Pritychenko, B.; Arbanas, G.; Arcilla, R.; et al. ENDF/B-VII.1 nuclear data for science and technology: Cross sections, covariances, fission product yields and decay data. *Nucl. Data Sheets* **2011**, *112*, 2887. Available online: <https://www.sciencedirect.com/science/article/pii/S009037521100113X> (accessed on 1 May 2024). [CrossRef]
9. Williams, M.L.; Wiarda, D.; Kim, K.S.; Jessee, M.A. Multigroup Data Processing for the Embedded Self-Shielding Method in SCALE. In Proceedings of the PHYSOR 2016, Sun Valley, ID, USA, 1–5 May 2016.
10. Kim, K.S.; Williams, M.L.; Wiarda, D.; Mertyurek, U. Automatic Coarse Energy Group Structure Optimization by Minimizing Reaction Rate Differences for the SCALE and CASL Code Systems. In Proceedings of the M&C 2017, Jeju, Republic of Korea, 16–20 April 2017.
11. Gavin, P.H. *Combustion Engineering Critical Experiments*; PH-68-3; ABB-CE: Windsor, TN, USA, 1968.
12. Kim, K.S. *Evaluation of Peaking Factors Uncertainty for CASMO-3*; KAERI/TR-628/96; Korea Atomic Energy Research Institute: Daejeon, Republic of Korea, 1996.
13. Newman, L.W.; Wittkopf, W.A.; Pettus, W.G.; Baldwin, M.N.; Hassan, H.A.; Uotinen, V.O.; Connell, J.D.; Campbell, P.S. *Urania Gadolinia: Nuclear Model Development and Critical Experiment Benchmark*; BAW-1810; Babcock & Wilcox: New York, NY, USA, 1984.
14. Godfrey, A.T. *VERA Core Physics Benchmark Progression Problem Specifications*; CASL-U-2012-0131-004; Oak Ridge National Laboratory: Oak Ridge, TN, USA, 2014.
15. Kim, K.S.; Mertyurek, U.; Wieselquist, W.A. *Benchmark Calculation for the Watts Bar Unit 1 Cycles 1–3 Using the SCALE 6.3/Polaris–PARCS v3.4.2 Code Package*; ORNL/TM-2023/2981; Oak Ridge National Laboratory: Oak Ridge, TN, USA, 2023.
16. Horelik, N.; Herman, B.; Forget, B.; Smith, K. Benchmark for Evaluation and Validation of Reactor Simulations (BEAVRS), v1.0.1. In Proceedings of the M&C 2013, Sun Valley, ID, USA, 5–9 May 2013.
17. Carlson, R.W. *Reactor Core Physics Design and Operating Data for Cycles 1, 2, and 3 of Surry Unit 1 PWR Power Plant*; EPRI NP-79-2-LD; Electric Power Research Institute: Palo Alto, CA, USA, 1979.
18. Nuclear Associates International Corporation. *Reactor Core Physics Design and Operating Data for Cycles 1, 2, and 3 of Turkey Point Unit 3 PWR Power Plant*; EPRI NP-827; Electric Power Research Institute: Palo Alto, CA, USA, 1978.
19. Kim, K.S.; Jessee, M.A.; Wieselquist, W.A. *Pin Peaking Factor Uncertainty of the SCALE 6.3/Polaris through Benchmarking the LWR Critical Experiments*; ORNL/TM-2023/2979; Oak Ridge National Laboratory: Oak Ridge, TN, USA, 2023.
20. Kim, K.S.; Wieselquist, W.A. *Benchmark Calculation for the BEAVRS Cycles 1–2 Using the SCALE 6.3/Polaris–PARCS v3.4.2 Code Package*; ORNL/TM-2023/2977; Oak Ridge National Laboratory: Oak Ridge, TN, USA, 2023.
21. Jeon, B.K.; Kim, K.S.; Wieselquist, W.A. *Benchmark Calculation for the Surry Unit 1 Cycles 1–3 Using the SCALE 6.3/Polaris–PARCS v3.4.2 Code Package*; ORNL/TM-2023/3039; Oak Ridge National Laboratory: Oak Ridge, TN, USA, 2023.
22. Jeon, B.K.; Kim, K.S.; Wieselquist, W.A. *Benchmark Calculation for the Turkey Point Unit 3 Cycles 1–3 Using the SCALE 6.3/Polaris–PARCS v3.4.2 Code Package*; ORNL/TM-2023/3061; Oak Ridge National Laboratory: Oak Ridge, TN, USA, 2023.
23. Owen, D.B. *Factors for One-Sided Tolerance Limits for Variables Sampling Plans*; SCR-607; Sandia Corporation: Albuquerque, NM, USA, 1963.
24. Kochunas, B.; Collins, B.; Stimpson, S.; Salko, R.; Jabaay, D.; Graham, A.; Liu, Y.; Kim, K.S.; Wieselquist, W.; Godfrey, A.; et al. VERA core simulator methodology for PWR cycle depletion. *Nucl. Sci. Eng.* **2017**, *185*, 217–231. [CrossRef]

Disclaimer/Publisher’s Note: The statements, opinions and data contained in all publications are solely those of the individual author(s) and contributor(s) and not of MDPI and/or the editor(s). MDPI and/or the editor(s) disclaim responsibility for any injury to people or property resulting from any ideas, methods, instructions or products referred to in the content.